PAPER

Quantum dynamical speedup for correlated initial states

To cite this article: Alireza Gholizadeh *et al* 2023 *Commun. Theor. Phys.* **75** 075101

You may also like

- Qubit geodesics on the Bloch sphere from optimal-speed Hamiltonian evolutions
Carlo Cafaro and Paul M Alsing

- Remotely detecting the signal of a local decohering process in spin chains
Saikat Sur and V Subrahmanyam

- Trapping phenomenon of the parameter estimation in asymptotic quantum states
K Berrada

Quantum dynamical speedup for correlated initial states

Alireza Gholizadeh[1]**, Maryam Hadipour**[1] ⬤**, Soroush Haseli**[1,2] ⬤**,
Saeed Haddadi**[3] ⬤ **and Hazhir Dolatkhah**[4] ⬤

[1] Faculty of Physics, Urmia University of Technology, Urmia, Iran
[2] School of Physics, Institute for Research in Fundamental Sciences (IPM), P.O. Box 19395-5531,
Tehran, Iran
[3] Saeed's Quantum Information Group, P.O. Box 19395-0560, Tehran, Iran
[4] RCQI, Institute of Physics, Slovak Academy of Sciences, Dúbravská cesta 9, 84511 Bratislava, Slovakia

E-mail: soroush.haseli@uut.ac.ir

Abstract

The maximal evolution speed of any quantum system can be expressed by the quantum speed
limit time. In this paper, we consider a model in which the system has a correlation with the
environment. The influence of the initial correlation between the system and environment on the
quantum speed limit is investigated. It is shown that the appearance of non-Markovianity effects
causes the speedup of quantum evolution. Moreover, we demonstrate the dependence of
quantum dynamical speedup on the quantum coherence of the correlated initial state.

Keywords: quantum speed limit, non-Markovianity, correlated initial state, quantum coherence

(Some figures may appear in colour only in the online journal)

1. Introduction

The question of how fast a quantum system can transform
from an initial state to an orthogonal state is a starting point to
study the quantum speed limit (QSL). The main goal of this
study is to find the general bounds that exist for any system
which can be used to limit the time (from below) taken for the
state of a system to be distinguishable from its initial state.
The bounds are known as QSL time. Indeed, QSL time is the
shortest possible time for the evolution of the system from an
initial state to the final orthogonal state. The study of QSL
time has particular importance for quantum communication
[1], computation [2], metrology [3], and many other areas of
quantum physics. The QSL time can be used to obtain the
shortest time needed to charge the quantum battery [4] and it
is also used to find the minimum time required to implement
quantum gates in quantum computing [5]. In [6], using the
geometry of the quantum state space, the inverse QSL is
introduced and its application in quantum batteries is also
discussed.

The first results of the studies on QSL time for closed
quantum systems were presented by Mandelstam and Tamm
(MT) [7]. They showed that for an evolution generated by a

time-independent Hamiltonian, the shortest possible time for
the transformation of an initial pure state to its final ortho-
gonal state is bounded by

$$\tau \geqslant \frac{\pi\hbar}{2\Delta E},\tag{1}$$

where $\Delta E = \sqrt{\langle\psi|H^2|\psi\rangle - \langle\psi|H|\psi\rangle^2}$ is the standard devia-
tion of time-independent Hamiltonian H and $\hbar$ is the reduced
Planck constant. The key point of the MT bound (1) is its
dependence on the standard deviation of the system energy. A
lot of work has been done to extend the MT bound, however,
the most effective result has been obtained by Margolus and
Levitin (ML), who have presented the new bound as [8]

$$\tau \geqslant \frac{\pi\hbar}{2E},\tag{2}$$

where $E = \langle H \rangle$ is the average energy over the ground state of
the system. The bound in equation (2) is known as ML bound.
So, for unitary evolution that connects two pure and ortho-
gonal states, the bound for the QSL is not unique, and usually
a comprehensive bound can be introduced by combining MT

and ML bounds as follows

$$\tau \geqslant \max\left\{\frac{\pi\hbar}{2\Delta E}, \frac{\pi\hbar}{2E}\right\}. \tag{3}$$

In the practical scenario, real quantum systems interact with their surroundings, such systems are called open quantum systems [9, 10]. In recent years, the study of the QSL for open quantum systems has received much attention [11–28]. The geometric approach is usually used to obtain the desired bound for the QSL in open quantum systems. In [13], Taddei *et al* have introduced a bound for the QSL in open quantum systems by using Fisher information for the total Hilbert space of the system and its environment. Escher *et al* developed their results in [29]. The authors of [12] have used relative purity to introduce a QSL bound for open quantum systems. They showed that when the evolution is in the Lindblad form, the bound is equivalent to the MT bound. Moreover, Deffner and Lutz [11] have introduced a bound for the QSL using the Bures angle, which covers both MT and ML bounds. They also showed that the non-Markovian effects can speed up the quantum process. In recent years, due to the fact that it is difficult to access an initial pure state in practical scenarios, studying the QSL for mixed initial states has been the subject of some works ([30, 31]). In addition to providing different bounds, some works have been done on the issue of QSL, such as the dependence of QSL on the initial state [32], and many other works [33–51].

In this paper, a comprehensive bound is considered for the QSL based on the function of relative purity, which can be applied to any mixed initial state [31]. Based on this bound, we investigate the QSL for a correlated initial state. It is observed that the QSL depends on the non-Markovianity of the evolution, the amount of initial correlation between the system and the environment, and the initial coherence of the system. We show that in addition to the non-Markovian effects, the initial correlation between the system and the environment can speed up the evolution of the quantum system. Besides, we reveal that strengthening the coupling of the system with the environment enhances the bound on the QSL.

The work is organized as follows. In section 2, the main structure of the model that will be used in this work is presented. In section 3, the non-Markovian feature of the model and parameters that are effective in the non-Markovian evolution will be studied. In section 4, the QSL for a correlated initial state will be investigated. Finally, the results will be summarized in section 5.

2. Model

Here, we consider a model in which a two-level system $\mathcal{S}$ is coupled to its environment $\mathcal{R}$. In this model, just the pure decoherence of the qubit is considered as a mechanism for decoherence and the energy dissipation is ignored. The model can be described by the following Hamiltonian [52]

$$H = H_{\mathcal{S}} + H_{\mathcal{R}} + H_{SR}, \tag{4}$$

where $H_{\mathcal{S}} = \omega_0 \sigma_z$ indicates the Hamiltonian of the system

with ω_0 which is the qubit energy splitting, $H_{\mathcal{R}} = \int_0^\infty d\omega h(\omega) a^\dagger(\omega) a(\omega)$ is the environment Hamiltonian, and $H_{\mathcal{S}\mathcal{R}} = \int_0^\infty d\omega \sigma_z [g^*(\omega) a(\omega) + g(\omega) a^\dagger(\omega)]$ is the interaction Hamiltonian. In the above Hamiltonian, σ_z is the z-component of the Pauli matrix, $a(\omega)$ and $a^\dagger(\omega)$ are the bosonic annihilation and creation operators, respectively, $h(\omega)$ is the real-valued spectrum function which describes the environment, and $g(\omega)$ is the function that characterizes the coupling. The whole Hamiltonian can be rewritten in block-diagonal form as [53]

$$H = \text{diag}[H_+, H_-], \quad H_\pm = H_{\mathcal{R}} \pm H_{\mathcal{S}\mathcal{R}} \pm \omega_0 \mathbb{I}_{\mathcal{R}}, \tag{5}$$

where $\mathbb{I}_{\mathcal{R}}$ is the identity operator in the environment Hilbert space. The correlated initial state for the system environment can be written as

$$|\Psi(0)\rangle = c_e |e\rangle \otimes |\Omega_0\rangle + c_g |g\rangle \otimes |\Omega_\lambda\rangle, \tag{6}$$

where $|e\rangle$ and $|g\rangle$ describe the excited and ground states of the system respectively, c_g and c_e are two non-zero complex numbers that satisfy $|c_g|^2 + |c_e|^2 = 1$. Besides, $|\Omega_0\rangle$ and $|\Omega_\lambda\rangle$ are the states of the environment where $|\Omega_0\rangle$ denotes an environment ground state and

$$|\Omega_\lambda\rangle = \eta_\lambda^{-1}[(1-\lambda)|\Omega_0\rangle + \lambda D(f)|\Omega_0\rangle], \tag{7}$$

where $D(f) = \exp\left\{\int_0^\infty d\omega[f(\omega) a^\dagger(\omega) - f^*(\omega) a(\omega)]\right\}$ is the displacement operator for an arbitrary square-integrable function f. Considering that the state presented in Eq.(7) should be normalized $\langle\Omega_\lambda|\Omega_\lambda\rangle = 1$, the coefficient η_λ is obtained as follows

$$\eta_\lambda^2 = (1-\lambda)^2 + \lambda^2 + 2\lambda(1-\lambda)\text{Re}\langle\Omega_0|D(f)|\Omega_0\rangle. \tag{8}$$

Above, the term Re means the real part of a complex number. The parameter $\lambda \in [0, 1]$ specifies the initial entanglement between the system and the environment. If this value is $\lambda = 0$, it means that the system and the environment are initially uncorrelated, while for $\lambda = 1$ there exists the greatest possible entanglement between the system and the environment. By considering the initial state of the composite system (6), the state of the system-environment at time t can be written as follows

$$|\Psi(t)\rangle = c_e |e\rangle \otimes |\psi_+(t)\rangle + c_g |g\rangle \otimes |\psi_-(t)\rangle, \tag{9}$$

where $|\psi_+(t)\rangle = \exp(-iH_+ t)|\Omega_0\rangle$ and $|\psi_-(t)\rangle = \exp(-iH_- t)|\Omega_\lambda\rangle$. The reduced density matrix of the system $\rho_{\mathcal{S}}^\lambda(t)$ is obtained by giving partial trace over the environment as

$$\rho_{\mathcal{S}}^\lambda(t) = \text{tr}_{\mathcal{R}}[|\Psi(t)\rangle\langle\Psi(t)|], \tag{10}$$

with more details, the explicit form of the above density matrix is obtained as follows

$$\rho_{\mathcal{S}}^\lambda(t) = \begin{pmatrix} |c_e|^2 & c_e c_g^* \kappa_\lambda(t) \\ c_e^* c_g \kappa_\lambda^*(t) & |c_g|^2 \end{pmatrix}, \tag{11}$$

with

$$\kappa_\lambda(t) = \eta_\lambda^{-1} e^{-i2\omega_0 t} e^{-r(t)}[1 - \lambda + \lambda e^{-2i\Phi(t)} e^{s(t)}], \tag{12}$$

where [54, 55]

$$r(t) = 4 \int_0^\infty d\omega J^2(\omega)[1 - \cos(\omega t)],$$

$$s(t) = 2 \int_0^\infty d\omega J(\omega)f(\omega)[1 - \cos(\omega t)] - \frac{1}{2}\int_0^\infty d\omega f^2(\omega),$$

$$\Phi(t) = \int_0^\infty d\omega J(\omega)f(\omega)\sin(\omega t).$$

(13)

In the above equations, $f(\omega)$ and $J(\omega)$ are the real function and the effective spectral density of the environment respectively, which are given by

$$f(\omega) = \omega^{\frac{\nu-1}{2}}\exp(-\omega/2\omega_c),$$
$$J(\omega) = \sqrt{\alpha}\,\omega^{\frac{\mu-1}{2}}\exp(-\omega/2\omega_c),$$

(14)

where α is the positive constant that describes the system-environment coupling, ω_c is the cutoff frequency, and μ is the ohmicity parameter. Note that the three cases $-1 < \mu < 0$, $\mu = 0$, and $\mu > 0$ correspond to the sub-ohmic, ohmic, and super-ohmic environments, respectively [56]. To study the evolution of the system in the model, the dynamics can be examined in two cases: (*i*) sub-ohmic and ohmic environments and (*ii*) super-ohmic environments. From a fundamental point of view, it is preferable to consider the super-ohmic case $\mu > 0$. From (13), one can obtain the following equations for the super-ohmic environment

$$r(t) = 4\omega_c^\mu \alpha \Gamma(\mu)\left\{1 - \frac{\cos\left[\mu\arctan(\omega_c t)\right]}{(1 + \omega_c^2 t^2)^{\mu/2}}\right\},$$

$$s(t) = 2\omega_c^\chi \sqrt{\alpha}\,\Gamma(\chi)\left\{1 - \frac{\cos\left[\chi\arctan(\omega_c t)\right]}{(1 + \omega_c^2 t^2)^{\chi/2}}\right\} - \frac{\omega_c^\nu}{2}\Gamma(\nu),$$

$$\Phi(t) = \omega_c^\chi \sqrt{\alpha}\,\Gamma(\chi)\frac{\sin\left[\chi\arctan(\omega_c t)\right]}{(1 + \omega_c^2 t^2)^{\chi/2}},$$

(15)

where $\chi = \frac{\mu+\nu}{2}$, and $\Gamma(.)$ is the Euler gamma function.

3. Non-Markovianity

According to the structural features of the environment, the quantum evolution can be classified into two categories: (a) Markovian (without memory) and (b) non-Markovian (with memory). In the Markovian process, the environment acts as a waster for the system information and information sinks from the system into the environment. Actually, in Markovian evolution, information leaks from the system to the environment and there is no back-flow from the environment to the system. While there exists a back-flow of information from the environment to the system during the evolution in the non-Markovian case. Up to now, several computational criteria have been introduced for the qualitative study of the non-Markovianity of quantum evolution [57–72]. In [58], Breuer *et al* have used state distinguishability to quantify the degree of non-Markovianity. They have interpreted the increment of state distinguishability as the return of information from the environment to the system. In this work, based on the state distinguishability, the non-Markovian criterion is considered

as follows

$$N = \max_{\rho_{1,2}(0)} \int_{\sigma>0} dt\sigma(t).$$

(16)

In the above relation, $\sigma(t)$ is the time derivative of trace distance

$$\sigma(t) = \frac{d}{dt}D(\rho_1(t), \rho_2(t)),$$

(17)

where $D(\rho_1, \rho_2) = \frac{1}{2}\mathrm{tr}|\rho_1 - \rho_2|$ is the trace distance that quantifies the distinguishability between two quantum states ρ_1 and ρ_2 (note that $|A| = \sqrt{A^\dagger A}$ and $0 \leqslant D \leqslant 1$). It should be noted that for the whole dynamical semigroups and all time-dependent Markovian evolution, we possess $\sigma(t) \leqslant 0$ while for $\sigma(t) > 0$, the evolution is non-Markovian. In other words, it can be said that in non-Markovian evolution, distinguishability increases in some time intervals. From equation (16), it is clear that quantifying the degree of non-Markovianity needs the performance of an optimization process over all pairs of initial states $\rho_{1,2}(0)$.

In [73], it has been shown that the optimal state pairs are orthogonal. Therefore, orthogonal states $\rho_1^{\lambda=0}(0) = |+\rangle\langle+|$ and $\rho_2^{\lambda=0}(0) = |-\rangle\langle-|$, where $|\pm\rangle = (|e\rangle \pm |g\rangle)/\sqrt{2}$, can be considered optimal states. For these optimal states, the trace distance at time t is obtained as

$$D(\rho_1(t), \rho_2(t)) = |\kappa_{\lambda=0}(t)|^2,$$

(18)

where $\kappa_\lambda(t)$ is presented in equation (12).

Now, the effects of the ohmicity parameter μ and coupling constant α on the degree of non-Markovianity N are investigated. Figure 1 shows the degree of non-Markovianity as functions of μ, α, and ν with fixed values $\lambda = 0$ and $\omega_c = \omega_0 = 1$. In figure 1(a), non-Markovianity is represented as functions of μ and α with $\nu = 0.01$. As can be seen from this plot, for $\alpha \simeq 0.01$, the degree of non-Markovianity has its maximum value at $\mu \simeq 5$, but for $\mu > 6$ and $\mu < 1$, it is equal to zero for all values of α, indicating the Markovian dynamics. It can also be noticed that for different values of ohmicity parameter in a certain interval $1 \leqslant \mu \leqslant 6$, the degree of non-Markovianity decreases by increasing α.

Figure 1(b) represents the non-Markovianity as functions of α and ν with $\mu = 5$. We see that the degree of non-Markovianity has its maximum value for $\alpha = 0.01$. It can also be detected that for all values of ν, the degree of non-Markovianity decreases when the value of α decreases or increases from $\alpha = 0.01$. By comparing figures 1(a) and (b), one can conclude that to have a non-Markovian evolution for the considered model, it is enough to hold $\mu = 5$ and $\alpha = 0.01$, regardless of the value of ν. In a similar way, it can be said that for $\mu > 6$, the evolution is Markovian regardless of the values of α and ν.

4. Quantum speed limit

In this section, the QSL is investigated for our considered model. Due to the initial correlation between the system and the environment, it is not possible for the initial state of the system to be pure. So, to calculate the QSL, it should be considered that
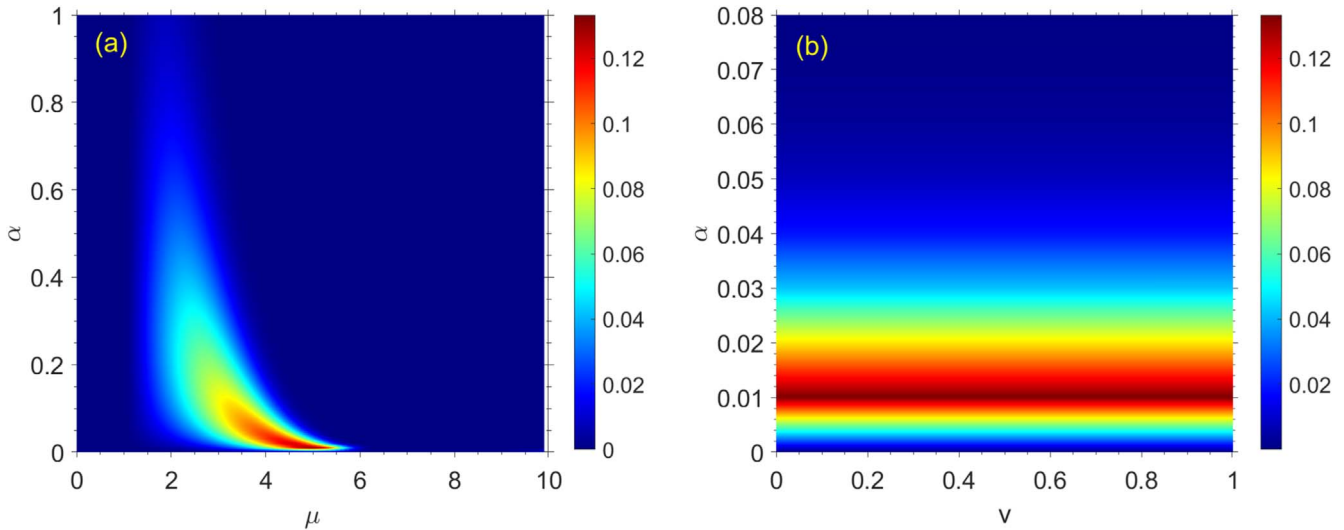
Figure 1. (a) Non-Markovianity *N* as a function of coupling constant α and ohmicity parameter μ with $v = 0.01$. (b) *N* as a function of α and v with $\mu = 5$. For two plots $\lambda = 0$ and $\omega_c = \omega_0 = 1$.

the initial state is mixed. In [30, 31], the authors have introduced QSL for the mixed initial states. Here, the method presented in [31] is used to study the QSL for the considered model.

The evolution of open quantum systems can be described by

$$\dot{\rho}_t = \mathcal{L}_t(\rho_t), \tag{19}$$

in which $\mathcal{L}_t$ denotes the time-dependent positive generator. In [31], the authors used the function of relative purity [74] as a distance measure, which is given by

$$\Theta(\rho_0, \rho_t) = \arccos\left(\sqrt{\frac{\mathrm{tr}[\rho_0\rho_t]}{\mathrm{tr}[\rho_0^2]}}\right). \tag{20}$$

Based on the above function, the ML-type QSL bound for open quantum systems can be obtained as [31]

$$\tau_{\mathrm{QSL}}^{\mathrm{ML}} = \max\left\{\frac{1}{\Lambda_\tau^{\mathrm{op}}}, \frac{1}{\Lambda_\tau^{\mathrm{tr}}}\right\} \sin^2\left[\Theta(\rho_0, \rho_\tau)\right]\mathrm{tr}[\rho_0^2], \tag{21}$$

with $\Lambda_\tau^{\mathrm{op(tr)}} = \frac{1}{\tau}\int_0^\tau \mathrm{d}t\,\|\mathcal{L}_t(\rho_t)\|_{\mathrm{op(tr)}}$, where $\|\mathcal{L}_t(\rho_t)\|_{\mathrm{tr}} = \sum_i \lambda_i$ and $\|\mathcal{L}_t(\rho_t)\|_{\mathrm{op}} = \lambda_1$ are the trace norm and operator norm for $\mathcal{L}_t(\rho_t)$. Herein, λ_i's and λ_1 are singular values and largest singular value of $\mathcal{L}_t(\rho_t)$.

Also, the MT-type bound on the QSL for non-unitary dynamics can be expressed as follows

$$\tau_{\mathrm{QSL}}^{\mathrm{MT}} = \frac{1}{\Lambda_\tau^{\mathrm{hs}}} \sin^2\left[\Theta(\rho_0, \rho_\tau)\right]\mathrm{tr}[\rho_0^2], \tag{22}$$

with $\Lambda_\tau^{\mathrm{hs}} = \frac{1}{\tau}\int_0^\tau \mathrm{d}t\,\|\mathcal{L}_t(\rho_t)\|_{\mathrm{hs}}$ where $\|\mathcal{L}_t\|_{\mathrm{hs}} = \sqrt{\sum_i \lambda_i^2}$ is the Hilbert-Schmidth norm of $\mathcal{L}_t(\rho_t)$. Combining equations (21) and (22), the unified bound on the QSL for non-unitary dynamics can be formulated as

$$\tau_{\mathrm{QSL}} := \max\left\{\frac{1}{\Lambda_\tau^{\mathrm{op}}}, \frac{1}{\Lambda_\tau^{\mathrm{tr}}}, \frac{1}{\Lambda_\tau^{\mathrm{hs}}}\right\} \sin^2\left[\Theta(\rho_0, \rho_\tau)\right]\mathrm{tr}[\rho_0^2]. \tag{23}$$

Notice that the ML-type bound based on the operator norm is the sharpest QSL bound for non-unitary dynamics.

Now, the QSL can be checked for the considered model. By putting $t = 0$ and $c_{e,g} = 1/\sqrt{2}$ in equation (11), the correlated initial state is obtained as

$$\rho_0 = \frac{1}{2}\begin{pmatrix} 1 & \kappa_\lambda(0) \\ \kappa_\lambda^*(0) & 1 \end{pmatrix}. \tag{24}$$

Hence, from equation (23), the QSL for the above correlated initial state can be obtained as

$$\tau_{\mathrm{QSL}} = \frac{|\kappa_\lambda(0)|^2 - |\kappa_\lambda(0)|\mathrm{Re}[\kappa_\lambda(\tau)]}{\int_0^\tau \mathrm{d}t\,|\dot{\kappa}_\lambda(t)|}, \tag{25}$$

where τ is the actual driving time.

In order to show the effect of initial quantum coherence of the correlated initial state on the QSL, it is necessary to consider an analytic quantifier of quantum coherence [75–79]. Here, the l_1-norm of coherence is considered to quantify the quantum coherence as $C(\rho) = \sum_{i\neq j}|\rho_{ij}|$. The l_1-norm quantum coherence of the correlated initial state (24) can be obtained as $C(\rho_0) = |\kappa_\lambda(0)|$. So, it can be seen that the initial quantum coherence depends on the initial correlation between the system and the environment, i.e., λ. The quantum coherence has its maximum value one for uncorrelated case $\lambda = 0$ and it is equal to zero for the fully correlated case $\lambda = 1$. Thus, the QSL in equation (25) can be rewritten as

$$\tau_{\mathrm{QSL}} = \frac{C(\rho_0)^2 - C(\rho_0)\mathrm{Re}[\kappa_\lambda(\tau)]}{\int_0^\tau \mathrm{d}t\,|\dot{\kappa}_\lambda(t)|}. \tag{26}$$

Figure 2 shows the changes of both QSL and non-Markovianity in terms of the ohmicity parameter μ. In figure 2(a), the QSL is sketched as a function of μ for correlated initial state $\lambda = 0.25$ with $v = \alpha = 0.01$ and driving time $\tau = 1$. Also, figure 2(b) represents the non-Markovianity in terms of μ with $\lambda = 0$ and $\alpha = v = 0.01$. Comparing plots 2(a) and (b), we find that there exists an inverse qualitative relationship between the QSL and non-Markovianity. Notably, for $\mu = 5$,
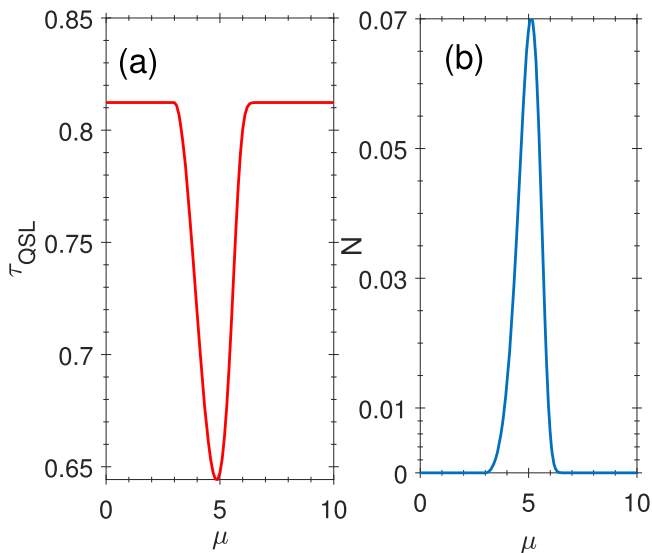
Figure 2. (a) QSL for a correlated initial state (24) as a function of ohmicity parameter μ with $\lambda = 0.25$ and $\tau = 1$. (b) Non-Markovianity in terms of μ with $\lambda = 0$. For two plots $\alpha = \nu = 0.01$, and $\omega_c = \omega_0 = 1$.
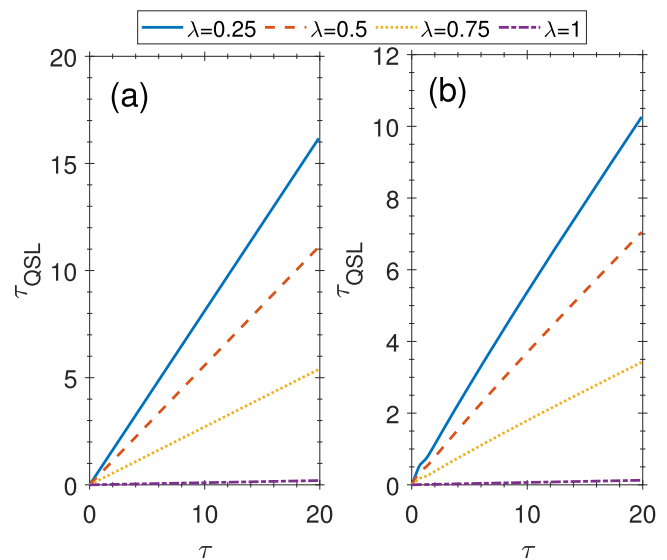

Figure 4. QSL as a function of driving time τ for different values of initial correlation between system and environment, $\lambda = 0.25, 0.50, 0.75,$ and 1. (a) Markovian regime $\mu = 8$ and (b) non-Markovian regime $\mu = 5$. For two plots $\alpha = \nu = 0.01$, and $\omega_c = \omega_0 = 1$.

the non-Markovian nature for $\mu = 5$, the QSL for both $\mu = 8$ and $\mu = 5$ coincide while, with the appearance of the non-Markovian nature at time $\tau = 0.58$, the QSL becomes shorter than the case with $\mu = 8$. Remarkably, it can be concluded that the non-Markovianity nature leads to the speedup of quantum evolution.

In figure 4, the QSL is illustrated as a function of driving time for different values of correlation parameter $\lambda = 0.25$, 0.50, 0.75, and 1 in both Markovian and non-Markovian regimes. These plots reveal the effect of initial correlation on the QSL in Markovian and non-Markovian cases. It can be found that for both Markovian and non-Markovian cases, the QSL will be shorter with increasing the initial correlation between the system and the environment.

In figure 5(a), the QSL is plotted as a function of correlation parameter λ with driving time $\tau = 1$. From figure 5(a), for both Markovian $\mu = 8$ and non-Markovian $\mu = 5$ evolutions, the QSL becomes shorter as the correlation parameter increases. As shown in equation (26), the QSL depends on the coherence of the initial state of the system. Therefore, to justify the result obtained from figure 5(a), the coherence of the initial state of the system is drawn in terms of λ in figure 5(b). As expected, the quantum coherence of the initial state of the system diminishes with increasing the correlation parameter λ.

In figure 6(a) the QSL is sketched as a function of coupling parameter α. As can be seen, the QSL grows with the increase of the coupling parameter α and reaches a constant value at $\alpha = 0.1$. Figure 6(b) represents the non-Markovianity in terms of coupling parameter α. Again, from plots 6(a) and (b) as well as figure 1, one can observe that in the non-Markovian regime ($\alpha \approx 0.01$), the QSL is shorter than in the Markovian case ($\alpha \approx 0.1$).

Finally, figure 7 displays the QSL as functions of the coupling parameter α and driving time τ for both Markovian

Figure 3. (a) QSL time as a function of driving time τ for both Markovian $\mu = 8$ and non-Markovian $\mu = 5$ environments with $\lambda = 0.25$. (b) Non-Markovianity versus τ for $\mu = 8$ and $\mu = 5$ with $\lambda = 0$. For two plots $\alpha = \nu = 0.01$, and $\omega_c = \omega_0 = 1$.

the degree of non-Markovianity has its maximum value, while the QSL has its minimum value (see also figure 1).

In figure 3, the QSL and non-Markovianity are plotted as a function of driving time τ. Figure 3(a) shows the QSL for both Markovian $\mu = 8$ and non-Markovian $\mu = 5$ environments. As can be seen, for the non-Markovian regime, the QSL is shorter than the Markovian regime. On the other hand, figure 3(b) illustrates the degree of non-Markovianity as a function of τ. As expected, the non-Markovianity is equal to zero for all driving time when $\mu = 8$. While for $\mu = 5$, the non-Markovian nature of the evolution is revealed from a specific driving time. An interesting result can be detected by comparing plots 3(a) and (b) is that before the appearance of
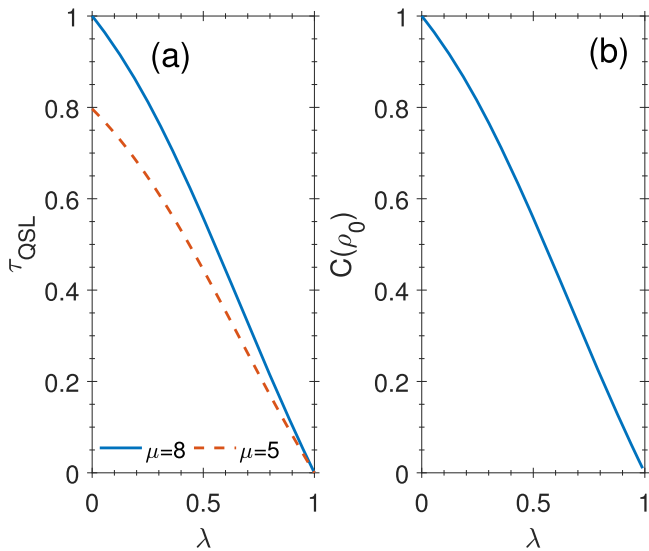
Figure 5. (a) QSL versus the correlation parameter λ for Markovian $\mu = 8$ and non-Markovian $\mu = 5$ regimes. (b) The l_1-norm of coherence $C(\rho_0)$ in terms of λ. For two plots $\alpha = v = 0.01$, $\omega_c = \omega_0 = 1$, and $\tau = 1$.
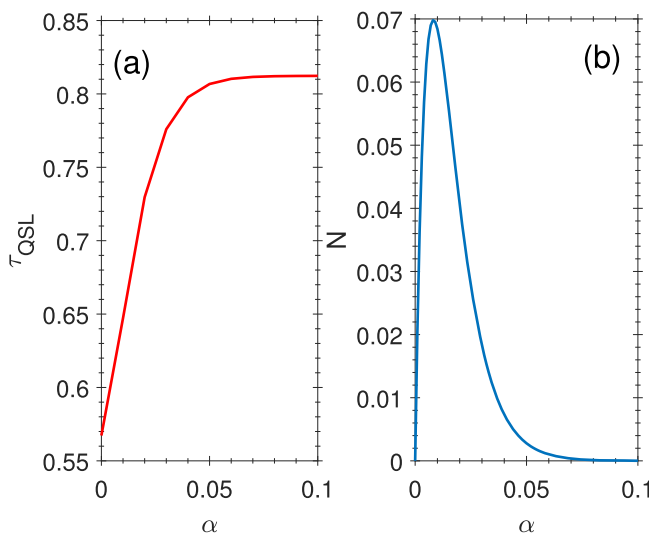

Figure 6. (a) QSL as a function of coupling parameter α for driving time $\tau = 1$ with $\lambda = 0.25$ and (b) non-Markovianity versus α with $\lambda = 0$. For two plots $v = 0.01$, $\omega_c = \omega_0 = 1$, and $\mu = 5$.

and non-Markovian dynamics when the correlation parameter is $\lambda = 0.25$. From figure 7(a), we find that the QSL does not alter with α changes for the Markovian case. However, figure 7(b) shows that in a non-Markovian regime, the QSL increases as α growths.

5. Conclusion

The QSL has been studied in an open quantum system with the initial correlation between the system and the environment. Specifically, we used the QSL bound based on the function of the relative purity introduced in [31]. First, we examined the considered model from the aspect of memory
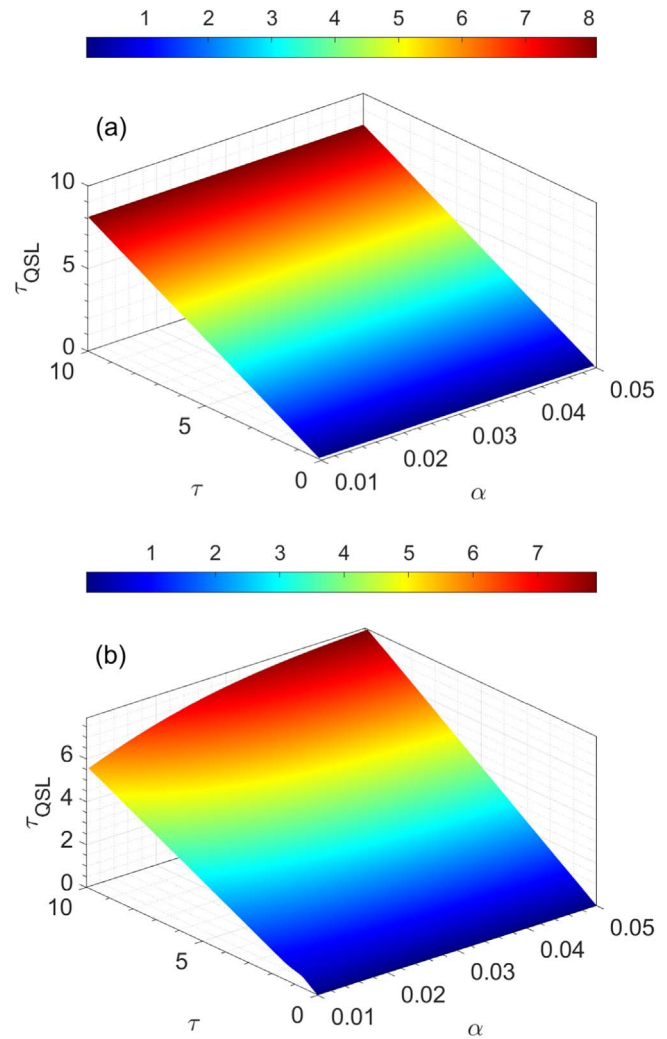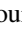

Figure 7. QSL as functions of coupling parameter α and driving time τ with $v = 0.01$, $\omega_c = \omega_0 = 1$, and $\lambda = 0.25$. (a) Markovian $\mu = 8$ (b) non-Markovian $\mu = 5$ regimes.

effects and determined the range of environmental parameters that cause the process to be non-Markovian. After that, we examined the effects of non-Markovianity of quantum evolution on QSL and found that the non-Markovian effects lead to shorter QSL. In other words, non-Markovian effects can speed up quantum evolution. We also observed that the initial coherence of the quantum system is directly related to the QSL, e.g., the highest QSL belongs to the initial states with the higher quantum coherence. As another result of this work, we found that increasing the initial correlation between the system and the environment leads to a decrease in the QSL. Indeed, the effect of the initial correlation between the system and environment on QSL originates from the dependence of QSL on quantum coherence. Moreover, we revealed that the increasing coupling parameter leads to a boost in QSL for the non-Markovian evolution.

Competing interests

The authors declare no competing interests.

ORCID iDs

Maryam Hadipour ⓘ https://orcid.org/0000-0002-6573-9960
Soroush Haseli ⓘ https://orcid.org/0000-0003-1031-4815
Saeed Haddadi ⓘ https://orcid.org/0000-0002-1596-0763
Hazhir Dolatkhah ⓘ https://orcid.org/0000-0002-2411-8690

References

[1] Bekenstein J D 1981 Energy cost of information transfer *Phys. Rev. Lett.* **46** 623
[2] Lloyd S 2000 Ultimate physical limits to computation *Nature* **406** 1047
[3] Giovannetti V, Lloyd S and Maccone L 2011 Advances in quantum metrology *Nature Photon* **5** 222
[4] Campaioli F, Pollock F A and Vinjanampathy S 2018 Quantum batteries *Thermodynamics in the Quantum Regime. Fundamental Theories of Physics* vol. 195 ed F Binder *et al* (Cham: Springer)
[5] Ashhab S, de Groot P C and Nori F 2012 Speed limits for quantum gates in multiqubit systems *Phys. Rev.* A **85** 052327
[6] Mohan B and Pati A K 2021 Reverse quantum speed limit: how slowly a quantum battery can discharge *Phys. Rev.* A **104** 042209
[7] Mandelstam L and Tamm I 1945 The uncertainty relation between energy and time in non-relativistic quantum mechanics *J. Phys. USSR* **9** 249
[8] Margolus N and Levitin L B 1998 The maximum speed of dynamical evolution *Physica* D **120** 188
[9] Breuer H P and Petruccione F 2002 *The Theory of Open Quantum Systems* (New York: Oxford University Press)
[10] Czerwinski A 2022 Dynamics of open quantum systems-Markovian semigroups and beyond *Symmetry* **14** 1752
[11] Deffner S and Lutz E 2013 Quantum speed limit for non-Markovian dynamics *Phys. Rev. Lett.* **111** 010402
[12] del Campo A, Egusquiza I L, Plenio M B and Huelga S F 2013 Quantum speed limits in open system dynamics *Phys. Rev. Lett.* **110** 050403
[13] Taddei M M, Escher B M, Davidovich L and de Matos Filho R L 2013 Quantum speed limit for physical processes *Phys. Rev. Lett.* **110** 050402
[14] Xu Z-Y and Zhu S-Q 2014 Quantum speed limit of a photon under non-Markovian dynamics *Chinese Phys. Lett.* **31** 020301
[15] Meng X, Wu C and Guo H 2015 Minimal evolution time and quantum speed limit of non-Markovian open systems *Sci. Rep.* **5** 16357
[16] Mirkin N, Toscano F and Wisniacki D A 2016 Quantum-speed-limit bounds in an open quantum evolution *Phys. Rev.* A **94** 052125
[17] Pires D P, Cianciaruso M, Céleri L C, Adesso G and Soares-Pinto D O 2016 Generalized geometric quantum speed limits *Phys. Rev.* X **6** 021031
[18] Jing J, Wu L A and Del Campo A 2016 Fundamental speed limits to the generation of quantumness *Sci. Rep.* **6** 38149
[19] Basilewitsch D, Schmidt R, Sugny D, Maniscalco S and Koch C P 2017 Beating the limits with initial correlations *New J. Phys.* **19** 113042
[20] Fischer J, Basilewitsch D, Koch C P and Sugny D 2019 Time-optimal control of the purification of a qubit in contact with a structured environment *Phys. Rev.* A **99** 033410
[21] Xu K, Zhang G-F and Liu W-M 2019 Quantum dynamical speedup in correlated noisy channels *Phys. Rev.* **100** 052305

[22] El Anouz K, El Allati A and Metwally N 2020 Different indicators for Markovian and non-Markovian dynamics *Phys. Lett.* A **384** 126122
[23] Awasthi N, Haseli S, Johri U C, Salimi S, Dolatkhah H and Khorashad A S 2020 Quantum speed limit time for correlated quantum channel *Quantum Inf. Process.* **19** 10
[24] Basilewitsch D, Fischer J, Reich D M, Sugny D and Koch C P 2021 Fundamental bounds on qubit reset *Phys. Rev. Research* **3** 013110
[25] Das A, Bera A, Chakraborty S and Chruściński D 2021 Thermodynamics and the quantum speed limit in the non-Markovian regime *Phys. Rev.* A **104** 042202
[26] García-Pintos L P, Nicholson S B, Green J R, del Campo A and Gorshkov A V 2022 Unifying quantum and classical speed limits on observables *Phys. Rev.* X **12** 011038
[27] Hadipour M, Haseli S, Dolatkhah H, Haddadi S and Czerwinski A 2022 Quantum speed limit for a moving qubit inside a leaky cavity *Photonics* **9** 875
[28] Shahri Y, Hadipour M, Haddadi S, Dolatkhah H and Haseli S 2023 Quantum speed limit of Jaynes–Cummings model with detuning for arbitrary initial states *Phys. Lett.* A **470** 128783
[29] Escher B M, de Matos Filho R L and Davidovich L 2011 General framework for estimating the ultimate precision limit in noisy quantum-enhanced metrology *Nature Phys.* **7** 406
[30] Zhang Y-J, Han W, Xia Y-J, Cao J-P and Fan H 2014 Quantum speed limit for arbitrary initial states *Sci. Rep.* **4** 4890
[31] Wu S-X and Yu C-S 2018 Quantum speed limit for a mixed initial state *Phys. Rev.* A **98** 042132
[32] Wu S-X, Zhang Y, Yu C-S and Song H-S 2015 The initial-state dependence of the quantum speed limit *J. Phys. A: Math. Theor.* **48** 045301
[33] Carabba N, Hörnedal N and del Campo A 2022 Quantum speed limits on operator flows and correlation functions *Quantum* **6** 884
[34] Xu Z Y 2016 Detecting quantum speedup in closed and open systems *New J. Phys.* **18** 073005
[35] Dehdashti S, Harouni M B, Mirza B and Chen H 2015 Decoherence speed limit in the spin-deformed boson model *Phys. Rev.* A **91** 022116
[36] Zhang Y-J, Han W, Xia Y-J, Cao J-P and Fan H 2015 Classical-driving-assisted quantum speed-up *Phys. Rev.* A **91** 032112
[37] Xu Z Y, Luo S, Yang W L, Liu C and Zhu S 2014 Quantum speedup in a memory environment *Phys. Rev.* A **89** 012307
[38] Mondal D and Pati A K 2016 Quantum speed limit for mixed states using an experimentally realizable metric *Phys. Lett.* A **380** 1395
[39] Ektesabi A, Behzadi N and Faizi E 2017 Improved bound for quantum-speed-limit time in open quantum systems by introducing an alternative fidelity *Phys. Rev.* A **95** 022115
[40] Sun Z, Liu J, Ma J and Wang X 2015 Quantum speed limits in open systems: non-Markovian dynamics without rotating-wave approximation *Sci. Rep.* **5** 8444
[41] Cai X and Zheng Y 2017 Quantum dynamical speedup in a nonequilibrium environment *Phys. Rev.* A **95** 052104
[42] Liu C, Xu Z Y and Zhu S 2015 Quantum-speed-limit time for multiqubit open systems *Phys. Rev.* **91** 022102 A
[43] Campaioli F, Chang-shui Y, Pollock A F and Modi K 2022 Resource speed limits: maximal rate of resource variation *New J. Phys.* **24** 065001
[44] Nakajima S and Utsumi Y 2022 Speed limits of the trace distance for open quantum system *New J. Phys.* **24** 095004
[45] Campbell C, Li J, Busch T and Fogarty T 2022 Quantum control and quantum speed limits in supersymmetric potentials *New J. Phys.* **24** 095001

[46] Aggarwal S, Banerjee S, Ghosh A and Mukhopadhyay B 2022 Non-uniform magnetic field as a booster for quantum speed limit: faster quantum information processing *New J. Phys.* **24** 085001

[47] Takahashi K 2022 Quantum lower and upper speed limits using reference evolutions *New J. Phys.* **24** 065004

[48] Mohan B, Das S and Pati A K 2022 Quantum speed limits for information and coherence *New J. Phys.* **24** 065003

[49] Lan K, Xie S and Cai X 2022 Geometric quantum speed limits for Markovian dynamics in open quantum systems *New J. Phys.* **24** 055003

[50] Hörnedal N, Allan D and Sönnerborn O 2022 Extensions of the Mandelstam–Tamm quantum speed limit to systems in mixed states *New J. Phys.* **24** 055004

[51] Aifer M and Deffner S 2022 From quantum speed limits to energy-efficient quantum gates *New J. Phys.* **24** 055002

[52] Dajka J and Łuczka J 2010 Distance growth of quantum states due to initial system-environment correlations *Phys. Rev. A* **82** 012341

[53] Spohn H and Lebowitz J L 1978 Irreversible thermodynamics for quantum systems weakly coupled to thermal reservoirs *Adv. Chem. Phys.* **38** 109

[54] Dajka J and Łuczka J 2008 Origination and survival of qudit–qudit entanglement in open systems *Phys. Rev. A* **77** 062303

[55] Dajka J, Mierzejewski M and Łuczka J 2009 Fidelity of asymmetric dephasing channels *Phys. Rev. A* **79** 012104

[56] Zhang Y-J, Han W, Xia Y-J, Yu Y-M and Fan H 2015 Role of initial system-bath correlation on coherence trapping *Sci. Rep.* **5** 13359

[57] Wolf M M, Eisert J, Cubitt T S and Cirac J I 2008 Assessing non-Markovian quantum dynamics *Phys. Rev. Lett.* **101** 150402

[58] Breuer H-P, Laine E-M and Piilo J 2009 Measure for the degree of non-Markovian behavior of quantum processes in open systems *Phys. Rev. Lett.* **103** 210401

[59] Rivas A, Huelga S F and Plenio M B 2010 Entanglement and non-Markovianity of quantum evolutions *Phys. Rev. Lett.* **105** 050403

[60] Hou S C, Yi X X, Yu S X and Oh C H 2011 Alternative non-Markovianity measure by divisibility of dynamical maps *Phys. Rev. A* **83** 062115

[61] Lu X-M, Wang X and Sun C P 2010 Quantum Fisher information flow and non-Markovian processes of open systems *Phys. Rev. A* **82** 042103

[62] Usha Devi A R, Rajagopal A K and Sudha 2011 Open-system quantum dynamics with correlated initial states, not completely positive maps, and non-Markovianity *Phys. Rev. A* **83** 022109

[63] Luo S, Fu S and Song H 2012 Quantifying non-Markovianity via correlations *Phys. Rev. A* **86** 044101

[64] Chruściński D and Maniscalco S 2014 Degree of non-Markovianity of quantum evolution *Phys. Rev. Lett.* **112** 120404

[65] He Z, Zeng H-S, Li Y, Wang Q and Yao C 2017 Non-Markovianity measure based on the relative entropy of coherence in an extended space *Phys. Rev. A* **96** 022106

[66] Bylicka B, Chruściński D and Maniscalco S 2014 Non-Markovianity and reservoir memory of quantum channels: a quantum information theory perspective *Sci. Rep.* **4** 5720

[67] Pineda C, Gorin T, Davalos D, Wisniacki D A and García-Mata I 2016 Measuring and using non-Markovianity *Phys. Rev. A* **93** 022117

[68] Rivas A, Huelga S F and Plenio M B 2014 Quantum non-Markovianity: characterization, quantification and detection *Rep. Prog. Phys.* **77** 094001

[69] Breuer H-P, Laine E-M, Piilo J and Vacchini B 2016 Colloquium: non-Markovian dynamics in open quantum systems *Rev. Mod. Phys.* **88** 021002

[70] Pollock F A, Rodríguez-Rosario C, Frauenheim T, Paternostro M and Modi K 2018 Operational Markov condition for quantum processes *Phys. Rev. Lett.* **120** 040405

[71] Costa F and Shrapnel S 2016 Quantum causal modelling *New J. Phys.* **18** 063032

[72] Pollock F A, Rodríguez-Rosario C, Frauenheim T, Paternostro M and Modi K 2018 Non-Markovian quantum processes: complete framework and efficient characterization *Phys. Rev. A* **97** 012127

[73] Wißmann S, Karlsson A, Laine E-M, Piilo J and Breuer H-P 2012 Optimal state pairs for non-Markovian quantum dynamics *Phys. Rev. A* **86** 062108

[74] Campaioli F, Pollock F A, Binder F C and Modi K 2018 Tightening quantum speed limits for almost all states *Phys. Rev. Lett.* **120** 060409

[75] Baumgratz T, Cramer M and Plenio M B 2014 Quantifying coherence *Phys. Rev. Lett.* **113** 140401

[76] Yu C S and Song H S 2009 Bipartite concurrence and localized coherence *Phys. Rev. A* **80** 022324

[77] Yu C S 2017 Quantum coherence via skew information and its polygamy *Phys. Rev. A* **95** 042337

[78] Zhao H and Yu C-S 2018 Coherence measure in terms of the Tsallis relative α entropy *Sci. Rep.* **8** 299

[79] Hu M-L, Hu X, Wang J, Peng Y, Zhang Y-R and Fan H 2018 Quantum coherence and geometric quantum discord *Phys. Rep.* **762-764** 1